

Inquiring electromagnetic quantum fluctuations about the orientability of space

C.H.G. Bessa,¹ N.A. Lemos,² and M.J. Rebouças³

¹*Departamento de Física, Universidade Federal de Campina Grande, Caixa Postal 5008
58429-900 Campina Grande – PB, Brazil*

²*Instituto de Física, Universidade Federal Fluminense, Av. Litorânea, S/N
24210-340 Niterói – RJ, Brazil*

³*Centro Brasileiro de Pesquisas Físicas, Rua Dr. Xavier Sigaud 150
22290-180 Rio de Janeiro – RJ, Brazil*

(Dated: January 20, 2022)

Abstract

Orientability is an important global topological property of spacetime manifolds. It is often assumed that a test for spatial orientability requires a global journey across the whole 3–space to check for orientation-reversing paths. Since such a global expedition is not feasible, theoretical arguments that combine universality of physical experiments with local arrow of time, CP violation and CPT invariance are usually offered to support the choosing of time- and space-orientable spacetime manifolds. In this paper, we show that it is possible to access spatial orientability of Minkowski empty spacetime through local physical effects involving quantum vacuum electromagnetic fluctuations. To this end, we study the motions of a charged particle and a point electric dipole subjected to these electromagnetic fluctuations in Minkowski spacetime with orientable and non-orientable spatial topologies. We derive analytic expressions for the velocity dispersion for both of these point-like particles in the two inequivalent spatially flat topologies. For the charged particle, we show that it is possible to distinguish the orientable from the non-orientable topology by contrasting the time evolution of the respective velocity dispersions. This is a significant result that makes apparent that it is possible to access orientability through electromagnetic quantum vacuum fluctuations. However, the answer to the central question of the paper, namely how to locally probe the orientability of Minkowski 3–space intrinsically comes about only in the study of the motions of an electric dipole. For this point-like particle, we find that a characteristic inversion pattern exhibited by the velocity dispersion curves is a signature of non-orientability. This important result makes it clear that it is possible to locally unveil spatial non-orientability through the inversion pattern of velocity dispersion curves of a point electric dipole under quantum vacuum electromagnetic fluctuations. Our findings open the way to a conceivable experiment involving quantum vacuum electromagnetic fluctuations to locally probe the spatial orientability on the microscopic scale of Minkowski empty spacetime.

PACS numbers: 03.70.+k, 05.40.Jc, 42.50.Lc, 04.20.Gz, 98.80.Jk, 98.80.Cq

I. INTRODUCTION

The Universe is modeled as a four-dimensional differentiable manifold, which is a topological space with an additional differential structure that permits to define locally connections, metric and curvature with which the gravitation theories are formulated. Geometry is a local attribute that brings about curvature, whereas topology is a global feature of a manifold related, for example, to compactness and orientability. Geometry constrains but does not specify the topology. So, topologically different manifolds can have a given geometry.¹

Since topology antecedes geometry, it is important to determine whether, how and to what extent physical phenomena depend upon or are somehow affected, induced, triggered, or even driven by a nontrivial topology. The net role played by the spatial topology is more clearly ascertained in the static spatially flat Friedmann-Lemaître-Robertson-Walker spacetime, whose dynamical degrees of freedom are frozen. Thus, in this work we focus on Minkowski spacetime, whose spatial geometry is Euclidean.

Although the topology of the spatial section, M_3 , of Minkowski spacetime, $\mathcal{M}_4 = \mathbb{R} \times M_3$, is usually taken to be the simply-connected Euclidean space \mathbb{E}^3 , it is a mathematical fact that it can also be any one of the possible 17 topologically distinct quotient (multiply-connected) manifolds $M_3 = \mathbb{E}^3/\Gamma$, where Γ is a discrete group of isometries or holonomies acting freely on the covering space \mathbb{E}^3 [8, 9]. The action of Γ tessellates or tiles the covering manifold into identical domains or cells which are copies of what is known as fundamental polyhedron (FP) or fundamental cell or domain (FC or FD). On the covering manifold \mathbb{E}^3 , the multiple connectedness of M_3 is taken into account by imposing periodic boundary conditions (repeated cells) that are determined by the action of the group of discrete isometries Γ on the covering space \mathbb{E}^3 .

In a manifold with periodic boundary conditions only certain modes of fields can exist. Thus, a nontrivial topology may leave its mark on the expectation values of local physical quantities. A case in point is the Casimir effect of topological origin [10–15].

Quantum vacuum fluctuations of the electromagnetic field in Minkowski spacetime seem

¹ Despite our present-day inability to predict the spatial topology of the Universe from a fundamental theory, one should be able to probe it through cosmic microwave background radiation (CMBR) or (and) stochastic primordial gravitational waves [1, 2], which should follow some basic detectability conditions [3]. For recent topological constraints from CMBR data we refer the readers to Refs. [4–6]. For some limits on the circles-in-the-sky method designed for the searches of cosmic topology through CMBR see Ref. [7].

not to produce observable effects on the motion of a charged test particle [16, 17]. However, when *changes* of topological nature in the background 3-space are made to allow for stochastic motions, as for example the insertion of perfectly reflecting planes into the three-dimensional spatial section, the resulting mean squared velocity of a charged test particle does not vanish [17–23].

In a recent paper, the question as to whether a nontrivial topology of the spatial section of Minkowski spacetime allows for stochastic motion of test charged particles under vacuum fluctuations of the electromagnetic field has been addressed [24]. It was shown that these vacuum fluctuations do indeed give rise to stochastic motions of charged particles as long as the spatial topology of Minkowski spacetime is nontrivial. In this way, either by inserting perfectly reflecting boundaries or by having any of the classified nontrivial 3-space topologies, the crucial background attribute to enable stochastic motions of charged particles under quantum vacuum electromagnetic fluctuations is a nontrivial 3-space topology of Minkowski spacetime.²

Orientability is an important global topological property of a spacetime manifold. It is widely assumed, implicitly or explicitly, that a manifold modeling the physical spacetime is globally orientable in all respects. Namely, that it is spacetime orientable and, additionally, that it is separately time and space orientable. Besides, it is also generally assumed that, being a global property, the 3-space orientability cannot be tested locally. Thus, to disclose the spatial orientability one would have to make a trip along some specific closed paths around the whole 3-space to check, for example, whether one returns with left- and right-hand sides exchanged. This reasoning is at first sight open to an intriguing criticism: since such a global journey across the whole 3-space is not feasible one might think that spatial orientability cannot be probed. In the face of this hurdle, one would have either to derive it from a fundamental theory of physics or answer the orientability question through cosmological observations or local experiments. Thus, it is conceivable that spatial orientability might be subjected to local experimental tests.³

² In Refs. [17–23] one has a nontrivial inhomogeneous quotient orbifold space topology while in Ref. [24] we have nontrivial flat smooth manifolds. We also note in this regard that the classification of three-dimensional Euclidean spaces was first taken up in the field of crystallography [26–28] and completed in 1934 [29]. For a recent exposition the reader is referred to Refs. [30–33].

³ One can certainly take advantage of gedanken experiments to reach theoretical conclusions, but not as a replacement to actual experimental evidence in physics [34].

Since quantum vacuum fluctuations of the electromagnetic field can be used to disclose a putative nontrivial 3-space topology of Minkowski spacetime through the velocity dispersion of the motions of test charged particles [24], and given that 8 out of the possible 17 quotient flat 3-manifolds are non-orientable [8], a question that naturally arises is whether these quantum vacuum fluctuations could be also used to reveal locally specific topological properties such as orientability of 3-space.⁴

Our chief goal in this article is to address this question by inquiring the electromagnetic quantum fluctuations about the spatial orientability of Minkowski spacetime. To this end, we investigate stochastic motions of a charged particle and of an electric dipole under quantum fluctuations of the electromagnetic field in Minkowski spacetime with two inequivalent spatial topologies, namely the orientable slab (E_{16}) and the non-orientable slab with flip (E_{17}).⁵ These topologies turn out to be suitable to show that one can unveil orientability and non-orientability signatures through the motion of point-like particles in Minkowski spacetime.

In Section II we introduce the notation and present some key concepts and results regarding topologies of three-dimensional manifolds, which will be needed in the rest of the paper. In Section III we present the physical systems along with the background geometry and topology, and derive the mean square velocity dispersion for motion of both a charged particle and an electric dipole under quantum vacuum electromagnetic fluctuations in Minkowski spacetime with E_{16} and E_{17} flat 3-space topologies. For the charged particle, we show that by comparing the time evolution of the velocity dispersions for a particle in E_{16} and E_{17} one can discriminate the orientable from the non-orientable topology. This result is significant in that it makes apparent the strength of our approach to access orientability through electromagnetic quantum vacuum fluctuations. However, the answer to the central question of the paper, namely how to locally probe the orientability of Minkowski 3-space per se, comes about only in the study of the stochastic motions of an electric dipole. In this regard, the most important finding is that the spatial non-orientability can be locally unveiled through the inversion pattern of velocity dispersion curves for a point electric dipole under quantum vacuum electromagnetic fluctuations. Section IV is dedicated to conclusions

⁴ In mathematical terms, this amounts to identifying signatures of non-translational covering holonomies through the motion of point-like particles under electromagnetic vacuum fluctuations.

⁵ In the next section we present a summary of flat three-dimensional topologies and some of their main topological properties. For a more detailed account on these topologies we recommend Refs. [30–33].

and final remarks.

II. TOPOLOGICAL PREREQUISITES

Our primary aim in this section is to introduce the notation and give some basic definitions and results concerning the topology of flat three-dimensional manifolds that are used throughout this paper. The spatial section M_3 of the Minkowski spacetime manifold $\mathcal{M}_4 = \mathbb{R} \times M_3$ is usually assumed to be the simply connected Euclidean space \mathbb{E}^3 .⁶ But it can also be a multiply-connected quotient 3-manifold of the form $M_3 = \mathbb{E}^3/\Gamma$, where \mathbb{E}^3 is the covering space and Γ is a discrete and fixed-point-free group of discrete isometries (also referred to as the holonomy group [8, 9]) acting freely on the covering space \mathbb{E}^3 [8].

Possibly the best known example of three-dimensional quotient Euclidean manifold with nontrivial topology is the 3-torus $T^3 = \mathbb{S}^1 \times \mathbb{S}^1 \times \mathbb{S}^1 = \mathbb{E}^3/\Gamma$, whose fundamental polyhedron (FP) is a parallelepiped with sides a, b, c (say), the opposite faces of which are identified through translations. In any multiply-connected quotient flat 3-manifold the fundamental polyhedron tiles (tessellates) the whole infinite simply-connected covering space \mathbb{E}^3 . The group $\Gamma = \mathbb{Z} \times \mathbb{Z} \times \mathbb{Z}$ consists of discrete translations associated with the face identification. The periodicities in the three independent directions are given by the circles \mathbb{S}^1 .

In forming the quotient manifolds M_3 an essential point is that they are obtained from the covering manifold \mathbb{E}^3 by identifying points that are equivalent under the action of the discrete isometry group Γ . Hence, each point on the quotient manifold M_3 represents all the equivalent points on the covering space. The multiple connectedness leads to periodic boundary conditions on the covering manifold \mathbb{E}^3 (repeated cells) that are determined by the action of the group Γ on the covering manifold. Clearly, different isometry groups Γ define different topologies for M_3 , which in turn give rise to different periodicity on the covering manifold (different mosaic of the covering space \mathbb{E}^3).

Another important point in forming the flat quotient manifolds M_3 is that every covering isometry $\gamma \in \Gamma$ can be expressed (in the covering space \mathbb{E}^3) through translation, rotation, reflection (flip) and combinations thereof. A screw motion, for example, is a combination of a rotation $R(\alpha, \hat{\mathbf{u}})$ by an angle α around an axis $\hat{\mathbf{u}}$, followed by a translation along a vector $\mathbf{L} = L \hat{\mathbf{w}}$, say. A general glide reflection is combination of a reflection followed by a

⁶ \mathbb{R}^3 is a topological space while \mathbb{E}^3 is a geometrical space, i.e. \mathbb{R}^3 endowed with the Euclidean metric.

translation, as for example $P = (x, y, z) \mapsto \gamma P = (-x, y, z) + (0, 0, c)$, where c is a constant. If $c = 0$ we have a simple reflection or flip.

In dealing with metric manifolds in mathematical physics two concepts of homogeneity arise. Local homogeneity is a geometrical characteristic of metric manifolds. It is formulated in terms of the action of the group of local isometries. In dealing with topological spaces, we have the global homogeneity of topological nature. A way to characterize global homogeneity of the quotient manifolds is through distance functions. Indeed, for any $\mathbf{x} \in M_3$ the distance function $\ell_\gamma(\mathbf{x})$ for a given discrete isometry $\gamma \in \Gamma$ is defined by

$$\ell_\gamma(\mathbf{x}) = d(\mathbf{x}, \gamma\mathbf{x}) , \quad (1)$$

where d is the Euclidean metric defined on M_3 . The distance function provides the length of the closed geodesic that passes through \mathbf{x} and is associated with a holonomy γ . In *globally homogeneous* manifolds the distance function for any covering isometry γ is constant. In globally inhomogeneous manifolds, in contrast, the length of the closed geodesic associated with at least one γ is non-translational (screw motion or flip, for example) and depends on the point $\mathbf{x} \in M_3$, and then is not constant.

When the distance between a point \mathbf{x} and its image $\gamma\mathbf{x}$ (in the covering space) is a constant for all points \mathbf{x} then the holonomy γ is a translation, that is, all elements of the covering group Γ in globally homogeneous spaces are translations. This means that in these manifolds the faces of the fundamental cells are identified through independent translations.

In this paper, we shall consider the topologically nontrivial spaces E_{16} and E_{17} . The slab space E_{16} is constructed by tessellating \mathbb{E}^3 by equidistant parallel planes, so it has only one compact dimension associated with a direction perpendicular to those planes. Taking the x -direction as compact, one has that, with $n_x \in \mathbb{Z}$ and $a > 0$, points (x, y, z) and $(x + n_x a, y, z)$ are identified in the case of the slab space E_{16} . The slab space with flip E_{17} involves an additional inversion of a direction orthogonal to the compact direction, that is, one direction in the tessellating planes is flipped as one moves from one plane to the next. Letting the flip be in the y -direction, the identification of points (x, y, z) and $(x + n_x a, (-1)^{n_x} y, z)$ defines the E_{17} topology. In this way, the slab space E_{16} is globally homogeneous, whereas the slab space with flip, E_{17} , is globally inhomogeneous since the covering group Γ contains a flip, which clearly is a non-translational discrete isometry.

Orientability is another very important global (topological) property of a manifold that

measures whether one can choose consistently a clockwise orientation for loops in the manifold. A closed curve in a manifold M_3 that brings a traveler back to the starting point mirror-reversed is called an orientation-reversing path. Manifolds that do not have an orientation-reversing path are called *orientable*, whereas manifolds that contain an orientation-reversing path are *non-orientable* [35]. Most surfaces that we encounter, such as cylinders, planes and tori are orientable, whereas the Möbius strip and Klein bottle are non-orientable surfaces. For three-dimensional quotient manifolds, when the covering group Γ contains at least an holonomy γ that is a reflection (flip) the corresponding quotient manifold is non-orientable. Thus, for example, the slab space is orientable while the slab space with flip is non-orientable. Clearly non-orientable manifolds are necessarily globally inhomogeneous as the covering group Γ contains a reflection, which obviously is a non-translational covering holonomy.

In Table I we collect the symbols and names used to refer to the manifolds together with the number of compact independent dimensions and information concerning their global homogeneity and orientability. These are the three-dimensional manifolds with nontrivial topologies that we shall be concerned with in this paper.

Symbol	Name	Compact Dim.	Orientable	Homogeneous
E_{16}	Slab space	1	yes	yes
E_{17}	Slab space with flip	1	no	no

TABLE I: Symbols and names of two multiply-connected flat orientable and non-orientable Euclidean quotient manifolds $M_3 = \mathbb{E}^3/\Gamma$ along with the number of compact dimensions, orientability and global (topological) homogeneity.

Having set the stage for our investigation, in the next section we proceed to show that the topological (global) non-orientability property of the spatial section of Minkowski spacetime manifold can be locally probed through the study of the motions of a charged test particle or a point electric dipole under quantum vacuum fluctuations of the electromagnetic field.

III. NON-ORIENTABILITY FROM ELECTROMAGNETIC FLUCTUATIONS

Quantum vacuum fluctuations of the electromagnetic field in Minkowski spacetime with nontrivial spatial topologies give rise to stochastic motions of charged particles. In this section, we address the main underlying question of this paper, which is whether these fluctuations offer a suitable way of discovering a putative non-orientability of Minkowski

3-space. We take up this question through the study of stochastic motions of a charged particle and an electric dipole under electromagnetic quantum fluctuations in Minkowski spacetime with two inequivalent spatial topologies, namely the orientable slab space (E_{16}) and the non-orientable slab space with flip (E_{17}). In the following we present the details of our investigation and main results.

A. NON-ORIENTABILITY WITH POINT CHARGED PARTICLE

We first consider a nonrelativistic test particle with charge q and mass m locally subjected to vacuum fluctuations of the electric field $\mathbf{E}(\mathbf{x}, t)$ in the topologically nontrivial spacetime manifold equipped with the Minkowski metric $\eta_{\mu\nu} = \text{diag}(+1, -1, -1, -1)$. The spatial section is usually taken to be \mathbb{E}^3 , but here we take for M_3 each of the two manifolds in Table I.

Locally, the motion of the charged test particle is determined by the Lorentz force. In the nonrelativistic limit the equation of motion for the point charge is

$$\frac{d\mathbf{v}}{dt} = \frac{q}{m} \mathbf{E}(\mathbf{x}, t), \quad (2)$$

where \mathbf{v} is the particle's velocity and \mathbf{x} its position at time t . We assume that on the time scales of interest the particle practically does not move (has a negligible displacement), so we can ignore the time dependence of \mathbf{x} . Thus, the particle's position \mathbf{x} is taken as constant in what follows [17, 23].⁷

Assuming that the particle is initially at rest ($t = t_0 = 0$) the integration of Eq. (2) gives

$$\mathbf{v}(\mathbf{x}, t) = \frac{q}{m} \int_0^t \mathbf{E}(\mathbf{x}, t') dt', \quad (3)$$

and the mean squared velocity, velocity dispersion or simply dispersion in each of the three independent directions $i = x, y, z$ is given by⁸

$$\langle \Delta v_i^2 \rangle = \frac{q^2}{m^2} \int_0^t \int_0^t \langle E_i(\mathbf{x}, t') E_i(\mathbf{x}, t'') \rangle dt' dt''. \quad (4)$$

Following Yu and Ford [17], we assume that the electric field is a sum of classical \mathbf{E}_c and quantum \mathbf{E}_q parts. Because \mathbf{E}_c is not subject to quantum fluctuations and $\langle \mathbf{E}_q \rangle = 0$, the

⁷ The corrections arising from the inexactness of this assumption are negligible in the low velocity regime.

⁸ By definition, $\langle \Delta \mathbf{v}^2(\mathbf{x}, t) \rangle \equiv \langle \mathbf{v}(\mathbf{x}, t) \cdot \mathbf{v}(\mathbf{x}, t) \rangle - \langle \mathbf{v}(\mathbf{x}, t) \rangle \cdot \langle \mathbf{v}(\mathbf{x}, t) \rangle$.

two-point function $\langle E_i(\mathbf{x}, t) E_i(\mathbf{x}', t') \rangle$ in equation (4) involves only the quantum part of the electric field [17].

It can be shown [36] that locally

$$\langle E_i(\mathbf{x}, t) E_i(\mathbf{x}', t') \rangle = \frac{\partial}{\partial x_i} \frac{\partial}{\partial x'_i} D(\mathbf{x}, t; \mathbf{x}', t') - \frac{\partial}{\partial t} \frac{\partial}{\partial t'} D(\mathbf{x}, t; \mathbf{x}', t') \quad (5)$$

where, in Minkowski spacetime with $M_3 = \mathbb{E}^3$, the Hadamard function $D(\mathbf{x}, t; \mathbf{x}', t')$ is given by

$$D_0(\mathbf{x}, t; \mathbf{x}', t') = \frac{1}{4\pi^2(\Delta t^2 - |\Delta \mathbf{x}|^2)}. \quad (6)$$

The subscript 0 indicates standard Minkowski spacetime, $\Delta t = t - t'$ and $|\Delta \mathbf{x}| \equiv r$ is the spatial separation for topologically trivial Minkowski spacetime:

$$r^2 = (x - x')^2 + (y - y')^2 + (z - z')^2. \quad (7)$$

In Minkowski spacetime with a topologically nontrivial spatial section, the spatial separation r^2 takes a different form that captures the periodic boundary conditions imposed on the covering space \mathbb{E}^3 by the covering group Γ , which characterize the spatial topology. In consonance with Ref. [12], in Table II we collect the spatial separations for the two topologically inequivalent Euclidean spaces we shall address in this paper.⁹

Spatial topology	Spatial separation r^2 for Hadamard function
E_{16} - Slab space	$(x - x' - n_x a)^2 + (y - y')^2 + (z - z')^2$
E_{17} - Slab space with flip	$(x - x' - n_x a)^2 + (y - (-1)^{n_x} y')^2 + (z - z')^2$

TABLE II: Spatial separation in Hadamard function for the multiply-connected flat orientable (E_{16}) and its non-orientable counterpart (E_{17}) quotient Euclidean manifolds. The topological compact length is denoted by a . The numbers n_x are integers and run from $-\infty$ to ∞ .

VELOCITY DISPERSION – SLAB SPACE WITH FLIP E_{17}

For the sake of brevity, we give here only the detailed calculations of the components of the velocity dispersion (4) for a charged particle in Minkowski spacetime with E_{17} spatial topology. The corresponding expressions for E_{16} spatial topology can then be easily obtained from those for E_{17} as we show below.

⁹ The reader is referred to Refs. [31–33] for pictures of the fundamental cells and further properties of all possible three-dimensional Euclidean topologies.

To obtain the correlation function for the electric field that is required to compute the velocity dispersion (4) for slab space with flip E_{17} , we replace in Eq. (5) the Hadamard function $D(\mathbf{x}, t; \mathbf{x}', t')$ by its renormalized version given by [24]

$$D_{ren}(\mathbf{x}, t; \mathbf{x}', t') = \sum_{n_x=-\infty}^{\infty'} \frac{1}{4\pi^2(\Delta t^2 - r^2)} \quad (8)$$

in which the prime indicates that the term of the sum with $n_x = 0$ is omitted, $\Delta t = t - t'$, and, from Table II, the spatial separation is

$$r^2 = (x - x' - n_x a)^2 + (y - (-1)^{n_x} y')^2 + (z - z')^2. \quad (9)$$

The term with $n_x = 0$ in the sum (8) that defines the renormalized Hadamard function $D_{ren}(\mathbf{x}, t; \mathbf{x}', t')$ has been subtracted out from the sum because it would give rise to an infinite contribution to the velocity dispersion.

Thus, from equation (5) the correlation functions

$$\langle E_i(\mathbf{x}, t) E_i(\mathbf{x}', t') \rangle = \frac{\partial}{\partial x_i} \frac{\partial}{\partial x'_i} D_{ren}(\mathbf{x}, t; \mathbf{x}', t') - \frac{\partial}{\partial t} \frac{\partial}{\partial t'} D_{ren}(\mathbf{x}, t; \mathbf{x}', t') \quad (10)$$

are then given by

$$\langle E_x(\mathbf{x}, t) E_x(\mathbf{x}', t') \rangle = \sum_{n_x=-\infty}^{\infty'} \frac{\Delta t^2 + r^2 - 2r_x^2}{\pi^2[\Delta t^2 - r^2]^3}, \quad (11)$$

$$\langle E_y(\mathbf{x}, t) E_y(\mathbf{x}', t') \rangle = \sum_{n_x=-\infty}^{\infty'} \frac{(3 - (-1)^{n_x}) \Delta t^2 + (1 + (-1)^{n_x}) r^2 - 4(-1)^{n_x} r_y^2}{2\pi^2[\Delta t^2 - r^2]^3}, \quad (12)$$

$$\langle E_z(\mathbf{x}, t) E_z(\mathbf{x}', t') \rangle = \sum_{n_x=-\infty}^{\infty'} \frac{\Delta t^2 + r^2 - 2r_z^2}{\pi^2[\Delta t^2 - r^2]^3}, \quad (13)$$

where $\Delta t = t - t'$ and

$$r_x = x - x' - n_x a, \quad r_y = y - (-1)^{n_x} y', \quad r_z = z - z', \quad r = \sqrt{r_x^2 + r_y^2 + r_z^2}. \quad (14)$$

The components of the velocity dispersion, given by Eq. (4), can then be computed with the help of the integrals [24]

$$I = \int_0^t \int_0^t dt' dt'' \frac{1}{(\Delta t^2 - r^2)^3} = \frac{t}{16r^5(t^2 - r^2)} \left\{ 4rt - 3(r^2 - t^2) \ln \frac{(r - t)^2}{(r + t)^2} \right\} \quad (15)$$

and

$$J = \int_0^t \int_0^t dt' dt'' \frac{\Delta t^2}{(\Delta t^2 - r^2)^3} = \frac{t}{16r^3(t^2 - r^2)} \left\{ 4rt + (r^2 - t^2) \ln \frac{(r - t)^2}{(r + t)^2} \right\}, \quad (16)$$

in which $\Delta t = t' - t''$.

Inserting equations (11) to (16) into Eq. (4) and taking the coincidence limit $\mathbf{x}' \rightarrow \mathbf{x}$ we find

$$\langle \Delta v_x^2 \rangle_{E_{17}} = \sum_{n_x=-\infty}^{\infty} \frac{q^2 t}{16\pi^2 m^2 r^5 (t^2 - r^2)} \left\{ 4rt(\bar{r}_x^2 + r^2) + (t^2 - r^2)(3\bar{r}_x^2 - r^2) \ln \frac{(r-t)^2}{(r+t)^2} \right\}, \quad (17)$$

$$\begin{aligned} \langle \Delta v_y^2 \rangle_{E_{17}} = \sum_{n_x=-\infty}^{\infty} \frac{q^2 t}{32\pi^2 m^2 r^5 (t^2 - r^2)} & \left\{ 4rt(\bar{r}_y^2 + (3 - (-1)^{n_x})r^2) \right. \\ & \left. + (t^2 - r^2)[3\bar{r}_y^2 - (3 - (-1)^{n_x})r^2] \ln \frac{(r-t)^2}{(r+t)^2} \right\}, \quad (18) \end{aligned}$$

$$\langle \Delta v_z^2 \rangle_{E_{17}} = \sum_{n_x=-\infty}^{\infty} \frac{q^2 t}{16\pi^2 m^2 r^5 (t^2 - r^2)} \left\{ 4rt(\bar{r}_z^2 + r^2) + (t^2 - r^2)(3\bar{r}_z^2 - r^2) \ln \frac{(r-t)^2}{(r+t)^2} \right\}, \quad (19)$$

where

$$r = \sqrt{n_x^2 a^2 + 2(1 - (-1)^{n_x})y^2}, \quad (20)$$

$$\bar{r}_x^2 = r^2 - 2r_x^2 = -n_x^2 a^2 + 2(1 - (-1)^{n_x})y^2, \quad (21)$$

$$\begin{aligned} \bar{r}_y^2 &= (1 + (-1)^{n_x})r^2 - 8(-1)^{n_x}(1 - (-1)^{n_x})y^2 \\ &= (1 + (-1)^{n_x})n_x^2 a^2 + 8(1 - (-1)^{n_x})y^2, \end{aligned} \quad (22)$$

$$\bar{r}_z^2 = r^2 - 2r_z^2 = r^2, \quad (23)$$

with the use of equations (14) in the coincidence limit.

As can be seen from Eqs. (20) – (23), the summands in Eqs (17) – (19) are even functions of the sum index n_x , therefore each sum equals twice the corresponding sum over positive n_x only. Thus we can write the components of the velocity dispersion in the form

$$\langle \Delta v_x^2 \rangle_{E_{17}} = \sum_{n=1}^{\infty} \frac{q^2 t}{8\pi^2 m^2 r_n^5 (t^2 - r_n^2)} \left\{ 4r_n t(\xi_n^2 + r_n^2) + (t^2 - r_n^2)(3\xi_n^2 - r_n^2) \ln \frac{(r_n - t)^2}{(r_n + t)^2} \right\}, \quad (24)$$

$$\begin{aligned} \langle \Delta v_y^2 \rangle_{E_{17}} = \sum_{n=1}^{\infty} \frac{q^2 t}{16\pi^2 m^2 r_n^5 (t^2 - r_n^2)} & \left\{ 4r_n t[\eta_n^2 + (3 - (-1)^n)r_n^2] \right. \\ & \left. + (t^2 - r_n^2)[3\eta_n^2 - (3 - (-1)^n)r_n^2] \ln \frac{(r_n - t)^2}{(r_n + t)^2} \right\}, \quad (25) \end{aligned}$$

$$\langle \Delta v_z^2 \rangle_{E_{17}} = \sum_{n=1}^{\infty} \frac{q^2 t}{8\pi^2 m^2 r_n^5 (t^2 - r_n^2)} \left\{ 8r_n^3 t + 2(t^2 - r_n^2)r_n^2 \ln \frac{(r_n - t)^2}{(r_n + t)^2} \right\}, \quad (26)$$

where

$$r_n = \sqrt{n^2 a^2 + 2(1 - (-1)^n)y^2}, \quad (27)$$

$$\xi_n^2 = -n^2 a^2 + 2(1 - (-1)^n)y^2, \quad (28)$$

$$\eta_n^2 = (1 + (-1)^n)n^2 a^2 + 8(1 - (-1)^n)y^2. \quad (29)$$

Since r_n , ξ_n and η_n depend on y , it follows that all components of the velocity dispersion depend on the flipped coordinate which gives rise to non-orientability.

Before proceeding to E_{16} topology, we discuss the topological Minkowskian limit for the velocity dispersion in E_{17} . We begin by recalling that compact lengths associated with Euclidean quotient manifolds are not fixed. Different values of a correspond to different 3-manifolds with the same topology. By letting $a \rightarrow \infty$ the topological Minkowskian limit for the velocity dispersion is attained. From Eq. (27) it follows that letting $a \rightarrow \infty$ amounts to letting $r_n \rightarrow \infty$. For very large r_n each term of the sum (24) consists of a fraction whose numerator is dominated by a power of r_n not bigger than the fourth (the logarithmic term tends to zero as $r_n \rightarrow \infty$) whereas the denominator becomes proportional to r_n^7 . Therefore each term of the sum vanishes in the limit $a \rightarrow \infty$ and the dispersion $\langle \Delta v_x^2 \rangle$ is zero, which is the topological Minkowskian limit for the velocity dispersion of a charged particle in Minkowski spacetime with spatial topology E_{17} . The same argument shows that the other components of the velocity dispersion also vanish in the limit $a \rightarrow \infty$. This result makes it clear that the vanishing of the velocity dispersion in the topological Minkowskian limit also holds for the non-orientable and globally inhomogeneous E_{17} topology. This extends the results obtained in Ref. [24] for globally homogeneous and orientable topologies, such as E_{16} for instance.

VELOCITY DISPERSION – SLAB SPACE E_{16}

The factors of $(-1)^{n_x}$ that appear in equations (12) and (18) arise from derivatives with respect to y' in Eq. (10) contributed by the separation r given by Eq. (9). Hence, the results for E_{16} are immediately obtained from those for E_{17} by simply replacing $(-1)^n$ by 1

everywhere in Eqs. (24) to (29). This leads to

$$\langle \Delta v_x^2 \rangle_{E_{16}} = -\frac{q^2 t}{2\pi^2 m^2} \sum_{n=1}^{\infty} \frac{1}{n^3 a^3} \ln \frac{(na - t)^2}{(na + t)^2}, \quad (30)$$

$$\langle \Delta v_y^2 \rangle_{E_{16}} = \langle \Delta v_z^2 \rangle_{E_{16}} = \frac{q^2 t}{4\pi^2 m^2} \sum_{n=1}^{\infty} \left\{ \frac{4t}{n^2 a^2 (t^2 - n^2 a^2)} + \frac{1}{n^3 a^3} \ln \frac{(na - t)^2}{(na + t)^2} \right\}, \quad (31)$$

in agreement with the results obtained in [24, 25].

ANALYSIS OF THE RESULTS

The velocity dispersions are singular at $t = r_n$, where $r_n = na$ for E_{16} whereas it is given by Eq. (27) for E_{17} . These singularities correspond to the time light takes to travel each of the infinitely many distances r_n that arise from the periodic boundary conditions imposed to take account of the identifications $(x, y, z) \leftrightarrow (x + n_x a, y, z)$ or $(x, y, z) \leftrightarrow (x + n_x a, (-1)^{n_x} y, z)$ in the covering space \mathbb{E}^3 . In the case in which \mathbb{E}^3 is split into two identical domains by the presence of a reflecting plane (nontrivial quotient orbifold), the velocity dispersion exhibits only one singularity [17], which has been ascribed to the local properties of the physical system. Accordingly, the introduction of a function of time to switch on and off the interaction between the particle and the electromagnetic field has been suggested to regularize the singularity [21, 23, 37]. This does not seem appropriate to cope with singularities that arise from global topological features of spacetime. Nevertheless, as remarked in [24], it may be possible to recast the switching function in terms of the topological parameter a (and presumably n_x) in order to smooth out the divergences with due regard to their topological origin. It is also conceivable that more realistic boundary conditions than those brought about by the method of images may be necessary to smear out the singularities. It is further to be noted that for both E_{16} and E_{17} the dispersions are negative for certain values of t . Therefore, an adequate regularization should render the velocity dispersions free of singularities and also positive. These are thorny issues that lie outside the purview of the present work, though.

A very important question that arises at this point is what then we ultimately learn from the above calculations regarding the local test of spatial orientability by studying the motions of a charged particle under electromagnetic quantum fluctuations. In other words, what these fluctuations are teaching us about orientability through velocity dispersions, equations (24) – (29) for the non-orientable E_{17} topology and equations (30) – (31) for

the orientable E_{16} space topology. Let us now discuss this capital issue. Clearly the chief conclusion can only be extracted through comparisons between the stochastic motions of the charged test particles lying in space manifolds with each of the two topologies. In this regard, a first difficulty one encounters is how to make a proper comparison because E_{16} is globally homogenous whereas E_{17} is not (cf. Table I). This means that the velocity dispersion does not depend on the particle's position for E_{16} , but it does when the particle lies in a space with the globally inhomogeneous topology E_{17} . The functional dependence of the dispersion on the particle's position coordinates in these manifolds makes apparent the first difficulty. Indeed, the components of the velocity dispersions (24) – (29) for E_{17} depend on the y -coordinate, while the components (30) – (31) for E_{16} do not. Thus, one has to suitably choose the point $P = (x, y, z)$ in E_{17} for the particle's position in order to make a proper comparison between the dispersions curves for the topologically homogeneous E_{16} and the topologically inhomogeneous E_{17} manifolds. From the identification of (x, y, z) and $(x + n_x a, (-1)^{n_x} y, z)$ that defines the E_{17} topology, clearly a suitable way to freeze out the global inhomogeneity degree of freedom, and thus isolate the non-orientability effect, is by choosing as the particle's position the point $P_0 = (x, 0, z)$. Since our chief concern is orientability, in all figures in this paper but one (Fig. 1) we choose this point as the particle's position when dealing with E_{17} topology.

Having circumvented this particle position difficulty related to the topological inhomogeneity of E_{17} , we illustrate in Fig. 1 how it affects the x -component curves of the normalized velocity dispersion

$$\langle \Delta \mathbf{v}^2(\mathbf{x}, t) \rangle_n \equiv \frac{m^2}{q^2} \langle \Delta \mathbf{v}^2(\mathbf{x}, t) \rangle. \quad (32)$$

For two particle's positions, one with $y = 0$ and another with $y = 1/2$ for compact length $a = 1$, in E_{17} one has different velocity dispersions curves. This shows that the velocity dispersion is able to capture the non-homogeneity of topological origin as has been indicated in [24]. By way of clarification, Figures 1 and 2 arise from Eqs. (24)–(29) as well as (30) and (31) with compact length $a = 1$ and n ranging from 1 to 50.

Figure 1 also shows that for the particle's position P_0 in E_{17} the dispersion curves coincide with those for a generic point in globally homogenous E_{16} . This shows that for $P_0 = (x, 0, z)$, where the global inhomogeneity degree of freedom is frozen, the x -component of the dispersion cannot be used to distinguish between the two orientable and non-orientable 3-spaces. With different pattern of curves, the same difficulty holds true for the z -components of the

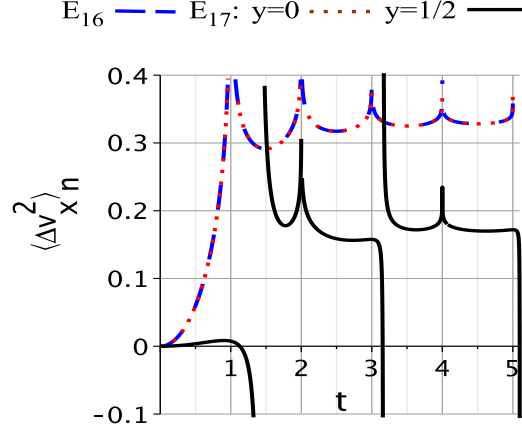


FIG. 1: Time evolution of the x -component of the normalized velocity dispersion $\langle \Delta \mathbf{v}^2(\mathbf{x}, t) \rangle_n$ for a test particle with mass m and charge q in Minkowski spacetime with spatial section endowed with the non-orientable and globally inhomogeneous E_{17} and orientable E_{16} topologies, both with compact length $a = 1$. We show one curve for the globally homogeneous E_{16} (dashed line) and two curves for E_{17} : dotted and solid lines, for the particle at the positions $P_0 = (x, 0, z)$ and $P = (x, 1/2, z)$, respectively. The figure illustrates the topological inhomogeneity of E_{17} , and shows that when the degree of inhomogeneity is frozen the dispersion curves for E_{17} [for the particle at $P_0 = (x, 0, z)$] and E_{16} [for the particle at generic $P = (x, y, z)$] coincide.

dispersion for E_{17} and E_{16} , but we do not show this figure for the sake of brevity. We note that this result on these two components of the dispersion are contained in our equations. Indeed, for the particle's position at $P_0 = (x, 0, z)$ for E_{17} , taking account of (27) – (29) it is straightforward to show that Eqs. (24) and (26) reduce, respectively, to (30) and (31). However, it should be noticed that even for $P_0 = (x, 0, z)$ the y -component of the dispersion $\langle \Delta v_y^2 \rangle_{E_{17}}$ does not reduce to $\langle \Delta v_y^2 \rangle_{E_{16}}$. This means that in order to extract information regarding orientability from the motion of a charged particle under electromagnetic fluctuations the proper comparison should be between the y -components of the dispersion, as we do in Fig. 2. This was to be expected from the outset since the reflection holonomy for E_{17} is in the y -direction (cf. Table II).

Figure 2 displays the y -components of the velocity dispersion of a charged test particle in Minkowski space whose spatial section has E_{16} (orientable) and E_{17} [non-orientable, $P_0 = (x, 0, z)$] topologies. Clearly the chief conclusion is that the component along the direction of the flip (cf. Table II) can be used to find out whether the particle lies in Minkowski spacetime with orientable or non-orientable 3-space. Figure 2 also shows different dispersion curves for E_{16} and E_{17} which, in both cases, repeat themselves periodically. For the two topologies

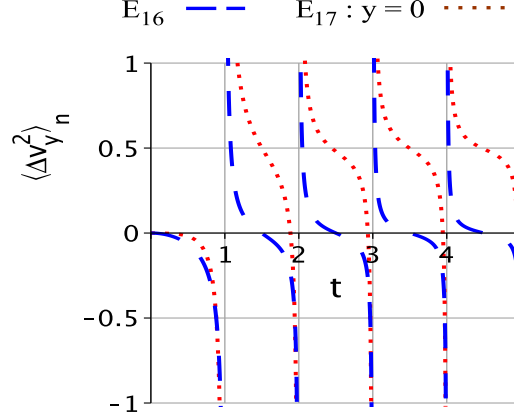


FIG. 2: Time evolution of the y -component of the normalized velocity dispersion for a charged test particle in Minkowski spacetime with spatial section endowed with the orientable E_{16} and non-orientable E_{17} topologies, both with compact length $a = 1$. We show curves for E_{16} (dashed line) and for E_{17} with the particle at $P_0 = (x, 0, z)$ (dotted line). The dispersion curves exhibit similar periodic patterns for time intervals of the order of one, but it is possible to distinguish the two topologies by contrasting the y -component of their velocity dispersions.

the overall patterns of the velocity dispersion curves are similar.

Although the above result is valuable to the extent that it makes clear the strength of our approach to access orientability through electromagnetic vacuum fluctuations, it demands a comparison between the dispersion curves for the two given spatial manifolds for a decision about orientability. Thus, it does not provide a conclusive answer to the central question of this paper, namely how to locally probe the orientability of the spatial section of Minkowski spacetime in itself through a physical experiment with electromagnetic vacuum fluctuations. Given the directional properties of a point electric dipole, a pertinent question that emerges here is whether it would be more effective to use it for testing the individual non-orientability of a generic 3-space. If so, after a suitable renormalization is worked out, we could envisage a local experiment to probe the orientability of a 3-space per se. In the next subsection we shall investigate this remarkable possibility.

B. NON-ORIENTABILITY WITH POINT ELECTRIC DIPOLE

A noteworthy outcome of the previous section is that the time evolution of the velocity dispersion for a charged particle can be used to locally differentiate an orientable (E_{16}) from a non-orientable (E_{17}) spatial section of Minkowski spacetime. However, it cannot be used to decide whether a given 3-space manifold is or not orientable. In this way, it

cannot be taken as a definite answer to our central question about the spatial orientability of Minkowski spacetime. So, a question that naturally arises here is whether the velocity dispersion of a different type of point-like particle could provide a suitable local signature of non-orientability. As a point electric dipole has directional properties, one would expect that its velocity dispersion could potentially bring about unequivocal information regarding non-orientability. To examine this issue we now turn our attention to topologically induced motions of an electric dipole under quantum vacuum electromagnetic fluctuations.

Newton's second law for a point electric dipole of mass m in an external electric field reads

$$m \frac{d\mathbf{v}}{dt} = \mathbf{p} \cdot \nabla \mathbf{E}(\mathbf{x}, t) \quad (33)$$

where \mathbf{p} is the electric dipole moment. With the same hypotheses as for the point charge and assuming the dipole is initially at rest, integration of Eq. (33) yields

$$\mathbf{v}(\mathbf{x}, t) = \frac{1}{m} p_j \int_0^t \partial_j \mathbf{E}(\mathbf{x}, t') dt' \quad (34)$$

with $\partial_j = \partial/\partial x_j$ and summation over repeated indices implied.

The mean squared speed in each of the three independent directions $i = x, y, z$ is given by

$$\langle \Delta v_i^2 \rangle = \frac{p_j p_k}{m^2} \int_0^t \int_0^t \langle (\partial_j E_i(\mathbf{x}, t')) (\partial_k E_i(\mathbf{x}, t'')) \rangle dt' dt'', \quad (35)$$

which can be conveniently rewritten as

$$\langle \Delta v_i^2 \rangle = \lim_{\mathbf{x}' \rightarrow \mathbf{x}} \frac{p_j p_k}{m^2} \int_0^t \int_0^t \partial_j \partial'_k \langle E_i(\mathbf{x}, t') E_i(\mathbf{x}', t'') \rangle dt' dt'' \quad (36)$$

where $\partial'_k = \partial/\partial x'_k$.

Now we proceed to the computation of the velocity dispersion for a point dipole in spaces E_{17} and E_{16} . The space E_{17} has two topologically conspicuous directions: the compact x -direction and the flip y -direction associated with the non-orientability of E_{17} . To probe the non-orientability of E_{17} by means of stochastic motions, it seems most promising to choose a dipole oriented in the y -direction, since the orientation of the dipole would also be flipped upon every displacement by the topological length a along the compact direction. Indeed, it is for a dipole oriented in the flip direction that the effect of the non-orientability is most noticeable, as we show in the following.

For a dipole oriented along the y -axis we have $\mathbf{p} = (0, p, 0)$ and

$$\langle \Delta v_x^2 \rangle^{(y)} = \lim_{\mathbf{x}' \rightarrow \mathbf{x}} \frac{p^2}{m^2} \int_0^t \int_0^t \partial_y \partial_{y'} \langle E_x(\mathbf{x}, t') E_x(\mathbf{x}', t'') \rangle dt' dt'', \quad (37)$$

where the superscript within parentheses indicates the dipole's orientation. With the help of Eq. (11) the x -component of the velocity dispersion for the slab space with flip E_{17} takes the form

$$\langle \Delta v_x^2 \rangle_{E_{17}}^{(y)} = \lim_{\mathbf{x}' \rightarrow \mathbf{x}} \frac{p^2}{\pi^2 m^2} \sum_{n_x=-\infty}^{\infty'} \int_0^t \int_0^t dt' dt'' \partial_y \partial_{y'} \frac{\Delta t^2 + r^2 - 2r_x^2}{(\Delta t^2 - r^2)^3}. \quad (38)$$

with r defined by Eq. (9) and $\Delta t = t' - t''$, while r_x is given by Eq. (14). Making use of

$$\partial_y \partial_{y'} \frac{\Delta t^2 + r^2 - 2r_x^2}{(\Delta t^2 - r^2)^3} = -4(-1)^{n_x} \left[\frac{2}{(\Delta t^2 - r^2)^3} + 3 \frac{r^2 - r_x^2 + 6r_y^2}{(\Delta t^2 - r^2)^4} + 24 \frac{(r^2 - r_x^2)r_y^2}{(\Delta t^2 - r^2)^5} \right]. \quad (39)$$

we find

$$\langle \Delta v_x^2 \rangle_{E_{17}}^{(y)} = -\frac{4p^2}{\pi^2 m^2} \sum_{n_x=-\infty}^{\infty'} (-1)^{n_x} \left\{ 2I_1 + 3(r^2 - r_x^2 + 6r_y^2)I_2 + 24(r^2 - r_x^2)r_y^2 I_3 \right\}, \quad (40)$$

where, with $\Delta t = t' - t''$,

$$I_1 = I = \int_0^t \int_0^t \frac{dt' dt''}{(\Delta t^2 - r^2)^3} = \frac{t}{16} \left[\frac{4t}{r^4(t^2 - r^2)} + \frac{3}{r^5} \ln \frac{(r-t)^2}{(r+t)^2} \right], \quad (41)$$

$$I_2 = \int_0^t \int_0^t \frac{dt' dt''}{(\Delta t^2 - r^2)^4} = \frac{1}{6r} \frac{\partial I_1}{\partial r} = \frac{t}{96} \left[\frac{4t(9r^2 - 7t^2)}{r^6(t^2 - r^2)^2} - \frac{15}{r^7} \ln \frac{(r-t)^2}{(r+t)^2} \right], \quad (42)$$

$$I_3 = \int_0^t \int_0^t \frac{dt' dt''}{(\Delta t^2 - r^2)^5} = \frac{1}{8r} \frac{\partial I_2}{\partial r} = \frac{t}{768} \left[\frac{4t(57t^4 - 136r^2t^2 + 87r^4)}{r^8(t^2 - r^2)^3} + \frac{105}{r^9} \ln \frac{(r-t)^2}{(r+t)^2} \right]. \quad (43)$$

Similar calculations lead to

$$\begin{aligned} \langle \Delta v_y^2 \rangle_{E_{17}}^{(y)} = & -\frac{2p^2}{\pi^2 m^2} \sum_{n_x=-\infty}^{\infty'} (-1)^{n_x} \left\{ (5 - 3(-1)^{n_x})I_1 + 6[r^2 + (7 - 6(-1)^{n_x})r_y^2]I_2 \right. \\ & \left. + 48[r^2 - (-1)^{n_x}r_y^2]r_y^2 I_3 \right\} \end{aligned} \quad (44)$$

and

$$\langle \Delta v_z^2 \rangle_{E_{17}}^{(y)} = -\frac{4p^2}{\pi^2 m^2} \sum_{n_x=-\infty}^{\infty'} (-1)^{n_x} \left\{ 2I_1 + 3(r^2 + 6r_y^2)I_2 + 24r^2 r_y^2 I_3 \right\}. \quad (45)$$

Since the coincidence limit $\mathbf{x}' \rightarrow \mathbf{x}$ has been taken, it follows from Eq. (14) that in Eqs. (40) to (45) one must put

$$r = \sqrt{n_x^2 a^2 + 2(1 - (-1)^{n_x})y^2}, \quad r_x^2 = n_x^2 a^2, \quad r_y^2 = 2(1 - (-1)^{n_x})y^2. \quad (46)$$

It can be immediately checked that, as for the point charge, in the Minkowskian limit ($a \rightarrow \infty$) the velocity dispersion for a dipole is zero.

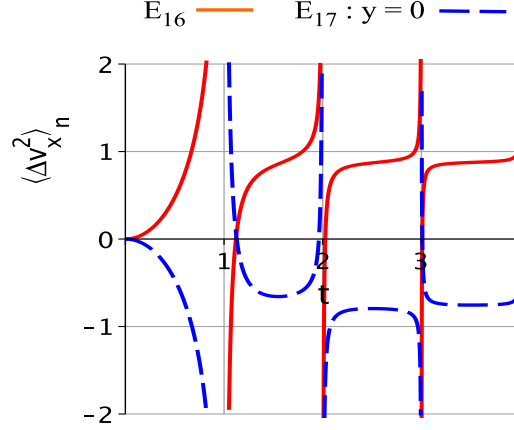


FIG. 3: Time evolution of the x -component of the normalized velocity dispersion $\langle \Delta \mathbf{v}^2(\mathbf{x}, t) \rangle_n$ for a point electric dipole oriented in the flip y -direction in Minkowski spacetime with orientable E_{16} and non-orientable E_{17} spatial topologies, both with compact length $a = 1$. The solid and dashed lines stand, respectively, for the dispersion curves for a dipole in 3-space with E_{16} and E_{17} topologies. For the globally inhomogeneous topology E_{17} the dipole is at $P_0 = (x, 0, z)$, thus freezing out the topological inhomogeneity. Both dispersion curves show a periodicity, but the curve for E_{17} exhibits a different kind of periodicity characterized by a distinctive inversion pattern. Non-orientability is responsible for this pattern of successive inversions, which is absent in the dispersion curve for the orientable E_{16} .

For the slab space E_{16} the components of the dipole velocity dispersion are obtained from those for E_{17} by setting $r_x^2 = r^2, r_y = 0$, and replacing $(-1)^{n_x}$ by 1 everywhere. Therefore, we have

$$\langle \Delta v_x^2 \rangle_{E_{16}}^{(y)} = -\frac{8p^2}{\pi^2 m^2} \sum_{n_x=-\infty}^{\infty}{}' I_1, \quad (47)$$

$$\langle \Delta v_y^2 \rangle_{E_{16}}^{(y)} = -\frac{4p^2}{\pi^2 m^2} \sum_{n_x=-\infty}^{\infty}{}' (I_1 + 3r^2 I_2), \quad (48)$$

$$\langle \Delta v_z^2 \rangle_{E_{16}}^{(y)} = -\frac{4p^2}{\pi^2 m^2} \sum_{n_x=-\infty}^{\infty}{}' (2I_1 + 3r^2 I_2), \quad (49)$$

in which $r = |n_x|a$.

ANALYSIS OF THE RESULTS

Now we ask ourselves what these fluctuations can reveal about spatial orientability through the velocity dispersion equations (40) – (45) for the dipole in the non-orientable 3-space with E_{17} topology, and equations (47) – (49) for the dipole in the orientable 3-space with E_{16} topology. In the remainder of this section we shall focus on this fundamental question.

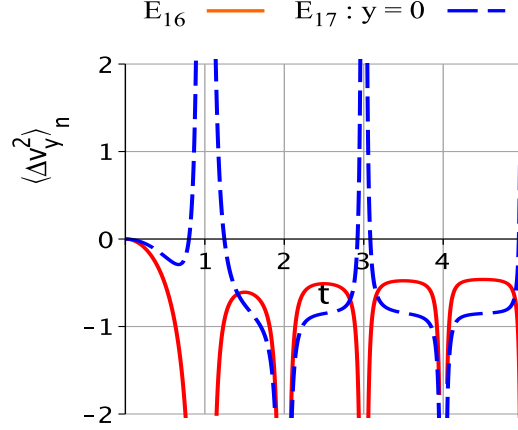


FIG. 4: Time evolution of the y -component of the normalized velocity dispersion for a point electric dipole oriented in the y -direction under the same conditions as those of Fig. 3. The velocity dispersion curve for E_{17} also displays a characteristic inversion pattern but which is different from the one for the x -component shown in Fig. 3. For the y -component of the velocity dispersion the signature of non-orientability can be recognized in the pattern of successive upward and downward “horns” formed by the dashed curve.

We begin by noting that the expressions for the components of the dispersion for E_{17} and E_{16} topologies are too involved to lend themselves to a straightforward interpretation. Nevertheless, something significant can be said: for a dipole located at $P_0 = (x, 0, z)$ all components of the velocity dispersion for E_{17} are different from those for E_{16} because each summand in Eqs. (40), (44) and (45) contains the prefactor $(-1)^{n_x}$ which is absent from the corresponding Eqs. (47) – (49) for E_{16} . Since not much further can be read from our equations, in order to demonstrate our main result, which is ultimately stated in terms of patterns of curves for the dispersion, we begin by plotting figures for the components of the velocity dispersion. Figures 3 to 5 come from Eqs. (40) – (45) as well as (47) – (49), with the topological length $a = 1$ and $n_x \neq 0$ ranging from -50 to 50 . The normalized velocity dispersion in these figures is defined by

$$\langle \Delta \mathbf{v}^2(\mathbf{x}, t) \rangle_n \equiv \frac{m^2}{p^2} \langle \Delta \mathbf{v}^2(\mathbf{x}, t) \rangle. \quad (50)$$

In the three figures the solid lines stand for the dispersion curves for the dipole in Minkowski spacetime with E_{16} orientable spatial topology, whereas the dashed lines indicate dispersion curves for the dipole located at $P_0 = (x, 0, z)$ in a 3-space with E_{17} non-orientable topology.

In the case of the x -component, the time evolution curves of the dispersion for E_{16} and E_{17} , shown in Fig. 3, present a common periodicity but clearly with distinguishable patterns. The dispersion curve for E_{17} displays a distinctive sort of periodicity characterized by an

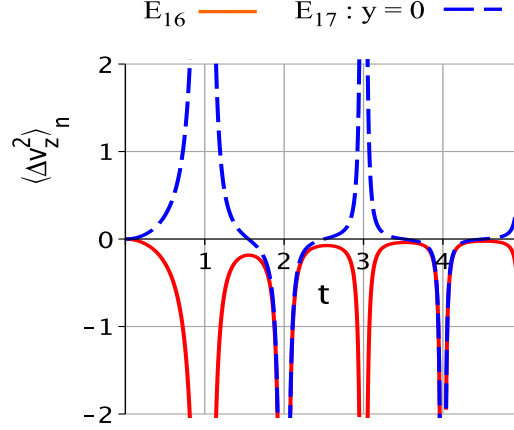


FIG. 5: Time evolution of the z -component of the normalized velocity dispersion for a point electric dipole oriented in the y -direction under the same conditions as those of Fig. 3. For the z -component of the velocity dispersion the non-orientability of E_{17} manifests itself by an inversion pattern similar to the one for the y -component shown in Fig. 4, namely the pattern of alternating upward and downward “horns” formed by the dashed curve.

inversion pattern. Non-orientability gives rise to this pattern of consecutive inversions, which is not present in the dispersion curve for the orientable E_{16} .

The differences become more salient when one considers the other two components of the velocity dispersion, shown in Figs. 4 and 5. For both of these components, the non-orientability of E_{17} is disclosed by an inversion pattern whose structure is more striking than the one for the x -component. The dispersion curves for E_{17} form a pattern of alternating upward and downward “horns”, making the non-orientability of E_{17} unmistakably identifiable.

From the above analysis of Figs. 3 to 5 as compared with the corresponding analysis of Fig. 2, we see that the point dipole is a much more efficient non-orientability probe than the point particle. Furthermore, the characteristic inversion pattern exhibited by the dipole dispersion curves makes it possible to identify the non-orientability of E_{17} by itself, without having to make a comparison with the dispersion curves for its orientable counterpart. We have checked, although we do not show the calculations, that for a dipole located at $P_0 = (x, 0, z)$ and oriented either in the x -direction or in the z -direction, only the y -component of the dispersion for E_{17} is different from the one for E_{16} . Thus, it is for a dipole oriented in the flip direction that the non-orientability of E_{17} is most sharply exposed.

This discussion leads us to the remarkable conclusion that it is possible to unveil a presumed spatial non-orientability by local means, namely by the stochastic motions of

point particles caused by quantum electromagnetic vacuum fluctuations. If the motion of a point electric dipole is taken as probe, non-orientability can be intrinsically discerned by the inversion pattern of the dipole's velocity dispersion curves.

IV. CONCLUSIONS AND FINAL REMARKS

In general relativity and quantum field theory spacetime is modeled as a differentiable manifold, which is a topological space equipped with an additional differential structure. Orientability is an important topological property of spacetime manifolds. It is often assumed that the spacetime manifold is orientable and, additionally, that it is separately time and space orientable. The theoretical arguments usually offered to assume orientability combine the space-and-time universality of local physical experiments¹⁰ with physically well-defined (thermodynamically, for example) local arrow of time, violation of charge conjugation and parity (CP violation) and CPT invariance [38–40]. One can certainly use such reasonings in support of the standard assumptions on the global structure of spacetime.¹¹ Nevertheless, it is reasonable to expect that the ultimate answer to questions regarding the orientability of spacetime should rely on cosmological observations or local experiments, or should even come from a fundamental theory of physics.

In the physics at daily and even astrophysical length and time scales, we do not find any sign or even hint of non-orientability. This being true, the remaining open question is whether the physically well-defined local orientations can be extended continuously to cosmological and/or microscopic scales.

At the cosmological scale, one would think at first sight that to disclose spatial orientability one would have to make a trip around the whole 3–space to check for orientation-reversing paths. Since such a global journey across the Universe is not feasible one might think that spatial orientability cannot be probed globally. However, a determination of the spatial topology through the so-called circles in the sky [43], for example, would bring out as a bonus an answer to the 3–space orientability problem at cosmological scale.¹²

¹⁰ This universality can be looked upon as a topological assumption of global homogeneity, which in turn rules out spatial non-orientability of 3–space.

¹¹ See Ref. [41] for a dissenting point of view, and also the related Ref. [42].

¹² In the searches for these circles so far undertaken, including the ones carried out by the Planck Collaboration [5, 6], no statistically significant pairs of matching circles have been found (see Ref. [4] for the most

In this paper we have addressed the question as to whether electromagnetic quantum vacuum fluctuations can be used to bring out on a microscopic scale the spatial orientability of Minkowski spacetime. To this end, we have studied the stochastic motions of point-like particles under quantum electromagnetic fluctuations in Minkowski spacetime with the orientable slab space (E_{16}) and the non-orientable slab space with flip (E_{17}) topologies (cf. Tables I and II).

For a point charged particle, we have derived analytic expressions for the velocity dispersion, namely Eqs. (24) – (29) for E_{17} space topology, and Eqs. (30) – (31) for E_{16} space topology. From these equations we have made Fig. 1 and Fig. 2. Using these equations and figures we have shown that it is possible to distinguish the orientable from the non-orientable topology by contrasting the time evolution of the respective velocity dispersions along the flip direction of E_{17} . In spite of being a significant result in that it makes apparent the power of our approach to access orientability through electromagnetic quantum vacuum fluctuations, it is desirable to be able to decide about the orientability of a given spatial manifold in itself. In this way, the results concerning the motion of a charged particle do not afford a conclusive answer to the central question posed in this paper, which is how to probe the orientability of Minkowski 3–space per se through a local physical experiment with electromagnetic vacuum fluctuations.

To tackle the central question, motivated by a dipole’s directional properties, we have then examined whether the study of stochastic motion of a point-like electric dipole would be more effective for testing the non-orientability of a generic 3–space individually, i.e. without having to make a comparison of the results for an orientable space with those for its non-orientable counterpart.

To this end, we have derived the velocity dispersion equations (40) – (45) for the dipole oriented in the flip direction in the non-orientable 3–space with E_{17} topology, and equations (47) – (49) for the dipole in the orientable 3–space with E_{16} topology. From these equations we have calculated and plotted Figures 3 to 5. As a result of the detailed analysis of these equations and figures we have found that there exists a characteristic inversion pattern exhibited by the velocity dispersion curves in the case of E_{17} , making apparent that the

extensive search yet, and also references therein for the other searches). These negative observational results, however, are not sufficient to exclude the possibility that the Universe has a detectable (orientable or non-orientable) nontrivial topology (see Ref. [7] for some limits of these searches).

non-orientability of E_{17} can be identified per se. The inversion pattern of the velocity dispersion curves for the dipole is ultimately a signature of the reflection holonomy, and ought to be present in the dispersion curves for the dipole in all remaining seven non-orientable topologies with flip, namely the four Klein spaces (E_7 to E_{10}) and those in the chimney-with-flip class (E_{13} to E_{15}).¹³ Clearly the inversion patterns for the electric dipole change with the associated topology: different topologies give rise to velocity dispersion curves with distinct inversion patterns.

Observation of physical phenomena and experiments are fundamental to our understanding the physical world. Our results make it clear that it is possible to locally unveil spatial non-orientability through the stochastic motions of point-like particles under electromagnetic quantum vacuum fluctuations. The present paper is a step on the way to a conceivable experiment involving these fluctuations to locally probe the spatial orientability of Minkowski empty spacetime.

Acknowledgments

M.J. Rebouças acknowledges the support of FAPERJ under a CNE E-26/202.864/2017 grant, and thanks CNPq for the grant under which this work was carried out. C.H.G. Bessa is funded by the Brazilian research agency CAPES. M.J.R. is also grateful to A.F.F. Teixeira for reading part of the manuscript and indicating typos.

-
- [1] G.F.R. Ellis, *Gen. Rel. Grav.* **2**, 7 (1971); M. Lachièze-Rey and J.P. Luminet, *Phys. Rep.* **254**, 135 (1995); G.D. Starkman, *Class. Quantum Grav.* **15**, 2529 (1998); J. Levin, *Phys. Rep.* **365**, 251 (2002); M.J. Rebouças and G.I. Gomero, *Braz. J. Phys.* **34**, 1358 (2004); M.J. Rebouças, A Brief Introduction to Cosmic Topology, in *Proc. XIth Brazilian School of Cosmology and Gravitation*, eds. M. Novello and S.E. Perez Bergliaffa (Americal Institute of Physics, Melville, NY, 2005) AIP Conference Proceedings vol. **782**, p 188, also: arXiv:astro-ph/0504365; J.P. Luminet, *Universe* 2016, 2(1), 1.
 - [2] M.J. Rebouças, *Detecting cosmic topology with primordial gravitational waves*, in preparation (2020).
 - [3] G.I. Gomero, M.J. Rebouças, and R. Tavakol, *Class. Quantum Grav.* **18**, 4461 (2001); G.I. Gomero, M.J. Rebouças, and Reza K. Tavakol, *Class. Quant. Grav.* **18**, L145 (2001); G.I. Gomero, M.J. Rebouças, and R. Tavakol, *Class. Quantum Grav.* **18**, L145 (2001); G.I. Gomero,

¹³ See Refs. [32, 33] for the symbols, names and properties of Klein spaces and chimney-with-flip families of non-orientable topologies.

- M.J. Rebouças, and R. Tavakol, *Int. J. Mod. Phys. A* **17**, 4261 (2002); J. Weeks, *Mod. Phys. Lett. A* **18**, 2099 (2003); B. Mota, M.J. Rebouças, and R. Tavakol, *Class. Quantum Grav.* **20**, 4837 (2003).
- [4] P.M. Vaudrevange, G.D. Starkman, N.J. Cornish, and D.N. Spergel, *Phys. Rev. D* **86**, 083526 (2012).
 - [5] P.A.R. Ade, *et al.* (Planck Collaboration 2013), *Astron. Astrophys.* **571**, A26 (2014).
 - [6] P.A.R. Ade *et al.* (Planck Collaboration 2015), *Astron. Astrophys.* **594**, A18 (2016).
 - [7] G. Gomero, B. Mota, and M.J. Rebouças, *Phys. Rev. D* **94**, 043501 (2016).
 - [8] J.A. Wolf, *Spaces of Constant Curvature* (McGraw-Hill, New York, 1967).
 - [9] W.P. Thurston, *Three-Dimensional Geometry and Topology. Vol.1*, Edited by Silvio Levy (Princeton University Press, Princeton, 1997).
 - [10] B.S. DeWitt, C.F. Hart and C.J. Isham, *Physica* **96A**, 197 (1979).
 - [11] J.S. Dowker and R. Critchley, *J. Phys. A* **9**, 535 (1976).
 - [12] P.M. Sutter and T. Tanaka, *Phys. Rev. D* **74**, 024023 (2006).
 - [13] M.P. Lima and D. Muller, *Class. Quant. Grav.* **24**, 897 (2007).
 - [14] D. Muller, H.V. Fagundes, and R. Opher, *Phys. Rev. D* **66**, 083507 (2002).
 - [15] D. Muller, H.V. Fagundes, and R. Opher, *Phys. Rev. D* **63**, 123508 (2001).
 - [16] C.H.G. Bessa, V.B. Bezerra, and L.H. Ford, *J. Math. Phys.* **50**, 062501 (2009).
 - [17] H. Yu and L.H. Ford, *Phys. Rev. D* **70**, 065009 (2004).
 - [18] H. Yu and J. Chen, *Phys. Rev. D* **70**, 125006 (2004).
 - [19] L.H. Ford, *Int. J. Theor. Phys.* **44**, 1753 (2005).
 - [20] H.W. Yu, J. Chen, and P. X. Wu, *JHEP* **0602**, 058 (2006).
 - [21] M. Seriu and C.H. Wu, *Phys. Rev. A* **77**, 022107 (2008).
 - [22] V. Parkinson and L.H. Ford, *Phys. Rev. A* **84**, 06210 (2011).
 - [23] V.A. De Lorenci, C.C.H. Ribeiro, and M. M. Silva, *Phys. Rev. D* **94**, 105017 (2016).
 - [24] C.H.G. Bessa and M.J. Rebouças, *Class. Quantum Grav.* **37**, 125006 (2020).
 - [25] J. Chen and H.W. Yu, *Chin. Phys. Lett.* **37**, 2362 (2004).
 - [26] E. Feodoroff, *Russ. J. Crystallogr. Mineral.* **21**, 1 (1885).
 - [27] L. Bieberbach, *Math. Ann.* **70**, 297 (1911).
 - [28] L. Bieberbach, *Math. Ann.* **72**, 400 (1912).
 - [29] W. Novacki, *Comment. Math. Helv.* **7**, 81 (1934).
 - [30] C. Adams and J. Shapiro, *American Scientist* **89**, 443 (2001).
 - [31] B. Cipra, *What's Happening in the Mathematical Sciences* (American Mathematical Society, Providence, RI, 2002).
 - [32] A. Riazuelo, J. Weeks, J.P. Uzan, R. Lehoucq, and J.P. Luminet, *Phys. Rev. D* **69**, 103518 (2004).
 - [33] H. Fujii and Y. Yoshii, *Astron. Astrophys.* **529**, A121 (2011).
 - [34] J. Anandan, *Phys. Rev. Lett.* **81**, 1363 (1998).
 - [35] J.R. Weeks, *The Shape of Space*, 3rd ed. (CRC Press, Boca Raton, FL, 2020).
 - [36] N.D. Birrel and P.C.W. Davies, *Quantum Fields in Curved Space* (Cambridge University Press, Cambridge, 1982).
 - [37] V.A. De Lorenci, and C.C.H. Ribeiro, *JHEP* **1904**, 072 (2019).
 - [38] Ya.B. Zeldovich and I.D. Novikov, *JETP Letters* **6**, 236 (1967).
 - [39] S.W. Hawking and G.F.R. Ellis, *The Large Scale Structure of Space-Time* (Cambridge University Press, Cambridge, 1973).
 - [40] R. Geroch and G.T. Horowitz, *Global structure of spacetimes* in General relativity: An Einstein centenary survey, pp. 212-293, Eds. S. Hawking and W. Israel (Cambridge University Press, Cambridge, 1979).

- [41] M. Hadley, Testing the Orientability of Time. Preprints 2018, 2018040240.
- [42] M. Hadley, Class. Quantum Grav. **19**, 4565 (2002).
- [43] N.J. Cornish, D. Spergel, and G. Starkman, Class. Quantum Grav. **15**, 2657 (1998).